COMMUNITY
COORDINATED
MODELING
CENTER

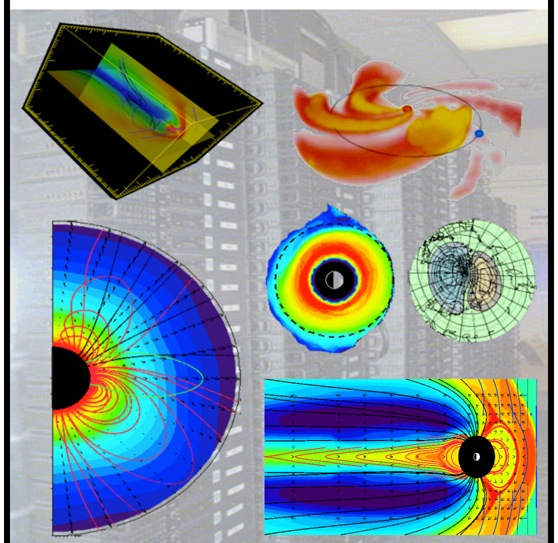

# Sensitivity of Ionosphere/Thermosphere to high-latitude drivers

**CCMC** : J. Shim, M. Kuznetsova, L. Rastäetter

**Modelers** : M. Codrescu, G. Crowley, B. Emery, M. Foerster, B. Foster, A. Namgaladze, A. Ridley, T. Fuller-Rowell, B. Prokhorov, M. Wiltberger

**Data providers** : A. Coster, L. Goncharenko, L. Lomidze, A. J. Mannucci, L. Scherliess, X. Pi

http://ccmc.gsfc.nasa.gov

NASA Goddard Space Flight Center

# Swapping of High-Latitude Drivers Using Kameleon

- CTIPe with SWMF electric potential since 2012 AGU
- Found memory leak of TIE-GCM with SWMF after 2013 GEM-CEDAR
- Fixed the memory leak issue in Mar. 2014

- CTIPe and TIE-GCM with electric potential and particle precipitation from
  - SWMF
  - AMIE

  in addition to their default models of electric potential and particle precipitation.

- More electric potential and particle precipitation models will be available.
- More IT models will be run with various drivers.

# Model Setting

| | Model Setting ID | |
|---|---|---|
| 1 | 1_CTIPe* | CTIPe driven with Weimer 2005 electric potential (EP) model and Fuller-Rowell & Evans particle precipitation (PP) model |
| 2 | 3_CTIPe* | CTIPe driven with high-latitude electric potential obtained from SWMF and Fuller-Rowell & Evans particle precipitation model |
| 3 | 3.1_CTIPe* | CTIPe driven with high-latitude electric potential (EP) and particle precipitation (PP) obtained from SWMF |
| 4 | 5_CTIPe* | CTIPe driven with AMIE_ASTRA (run with magnetometers, SuperDARN, and DMSP inputs) EP and Fuller-Rowell & Evans particle precipitation model |
| 5 | 5.1_CTIPe* | CTIPe driven with AMIE_ASTRA (run with magnetometers, SuperDARN, and DMSP inputs) EP and particle precipitation |
| 6 | 2_TIE-GCM* | TIE-GCM1.94 driven with Weimer 2005 EP and Roble & Ridley particle precipitation |
| 7 | 7_TIE-GCM* | TIE-GCM1.94 driven with AMIE_ASTRA EP and AMIE_ASTRA particle precipitation |
| 8 | 8_TIE-GCM* | TIE-GCM1.94 driven with SWMF EP and SWMF particle precipitation |
| 9 | 9_TIE-GCM | TIE-GCM1.94 driven with CMIT EP and CMIT particle precipitation |
| 10 | 1_UAM | Upper Atmosphere Model (UAM), A. A. Namgaladze et al., FAC as external driver |
| 11 | 2_UAM | UAM with AMIE_UM electric potentials as external drivers |
| 12 | 3_UAM | UAM with Weimer-2005 (and/or Weimer-96) electric potentials |

*Runs performed at the CCMC

# Electric Potential (northern hemisphere, 12/15/2006 00:00)

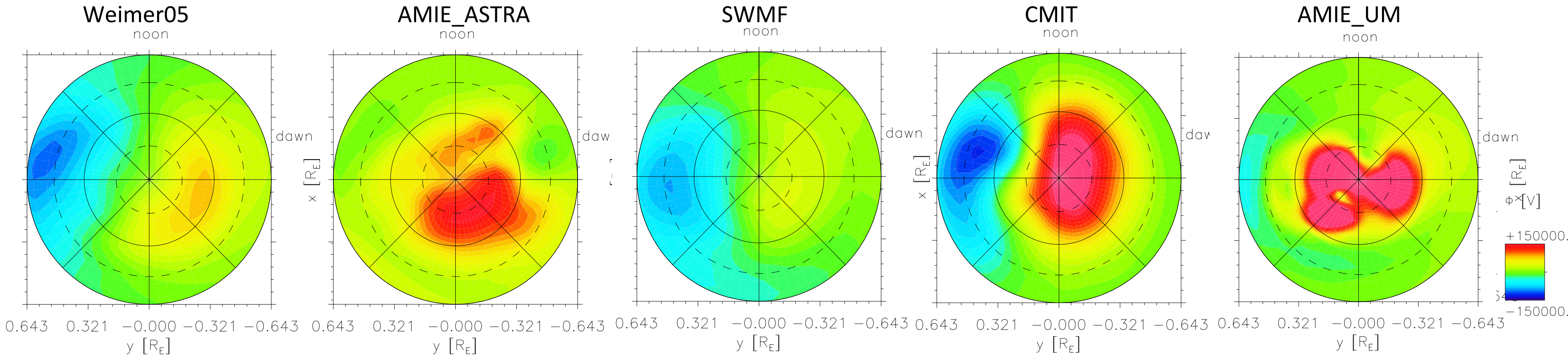


Min: -89.1 Max: 75.9 | Min:-83 Max: 150 | Min: -73.9 Max: 53.0 | Min:-165 Max: 204 | Min:-60 Max: 454

# Cross Polar Cap Potential (NH)

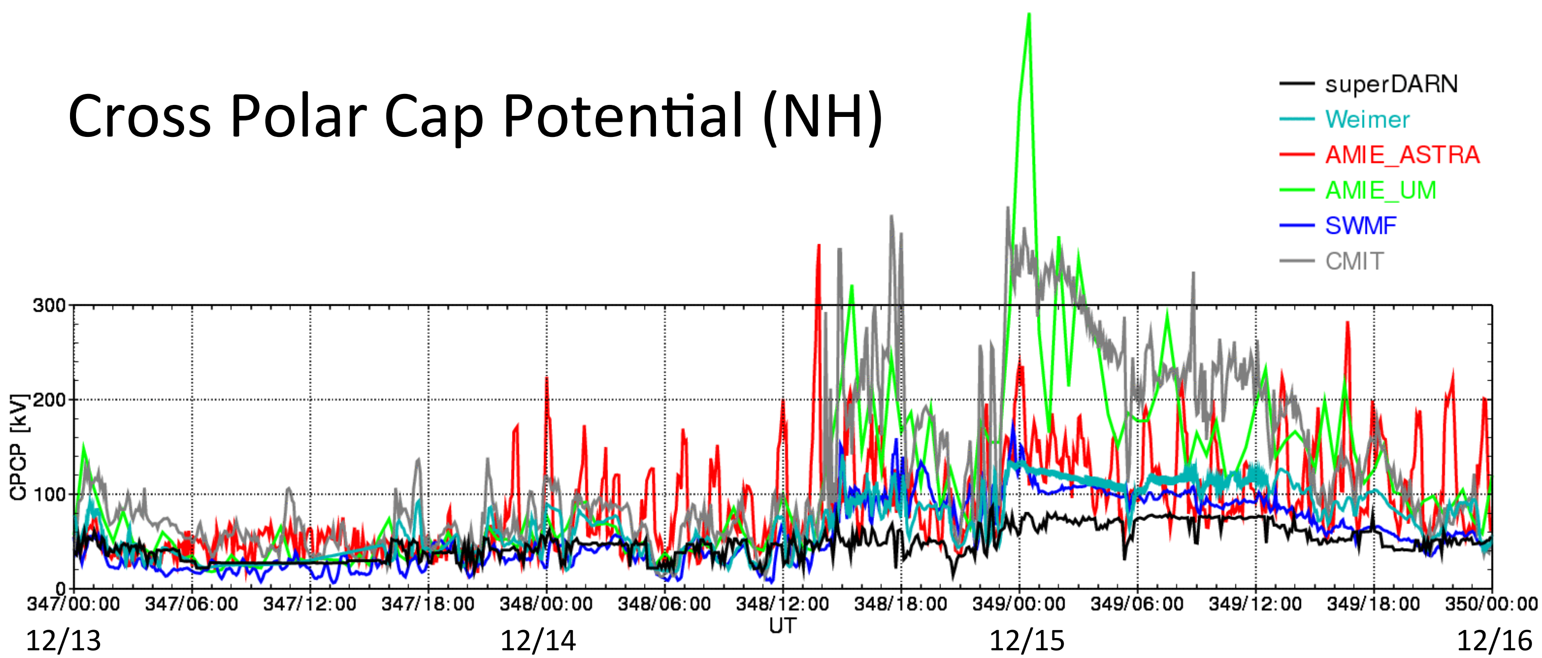

# Energy Flux (NH) (12/15/2006 00:00)

AMIE_ASTRA | SWMF | CMIT

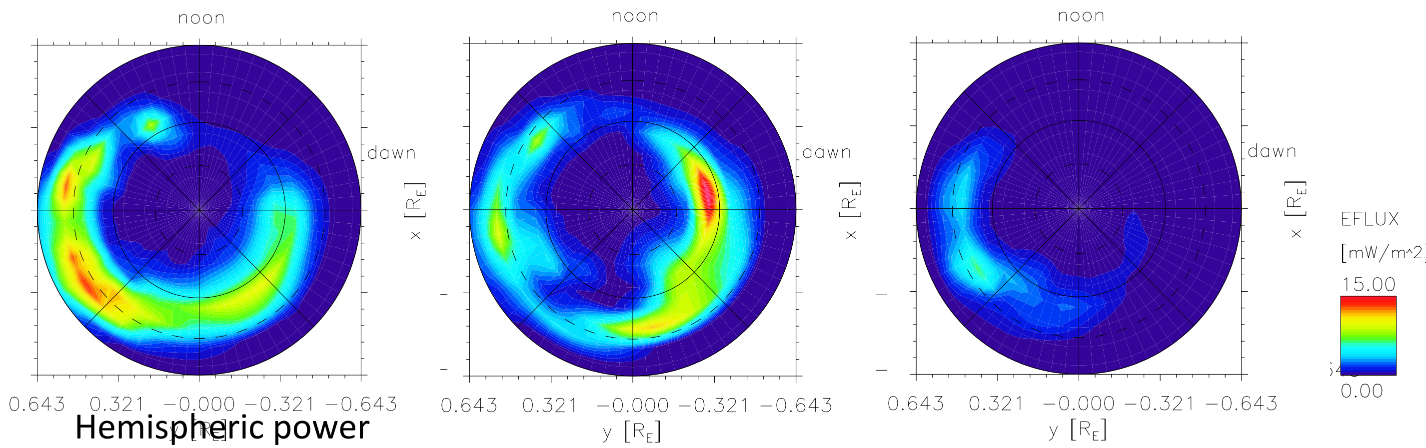


Hemispheric power

164 GW | 140 GW | 26 GW

- During storm time, energy flux and spatially integrated energy flux (hemispheric power: not shown here) obtained from AMIE_ASTRA is larger than those obtained from CMIT, while CMIT CPCP is larger than AMIE_ASTRA CPCP.

# Joule Heating (NH) (12/15/2006 00:00): CTIPe runs

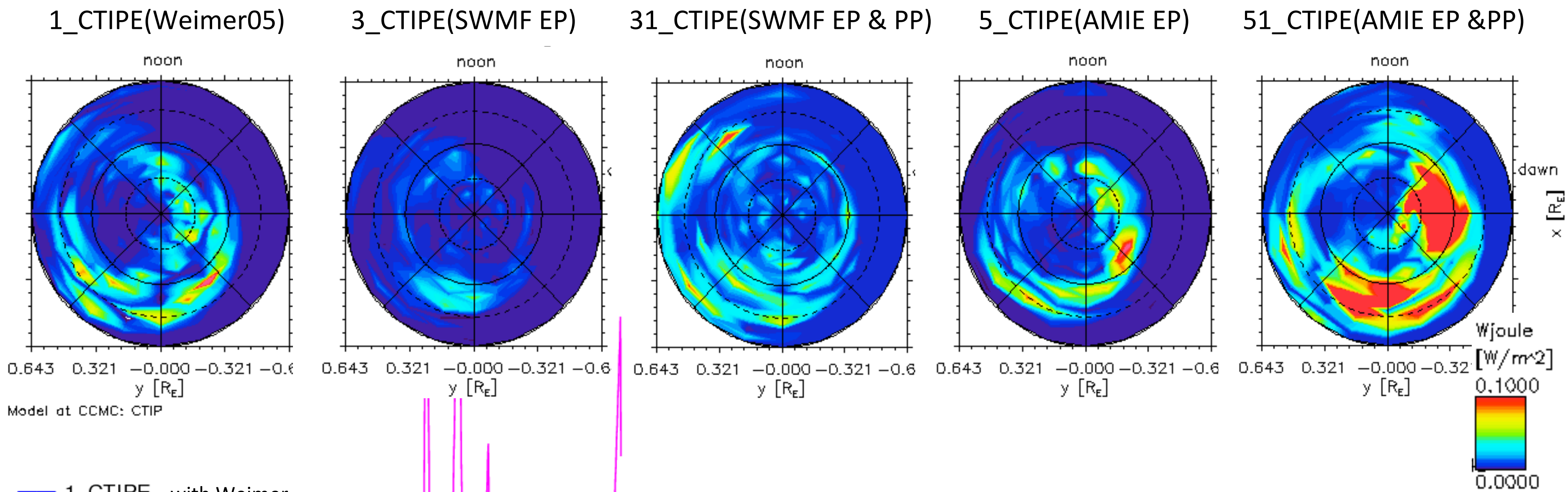


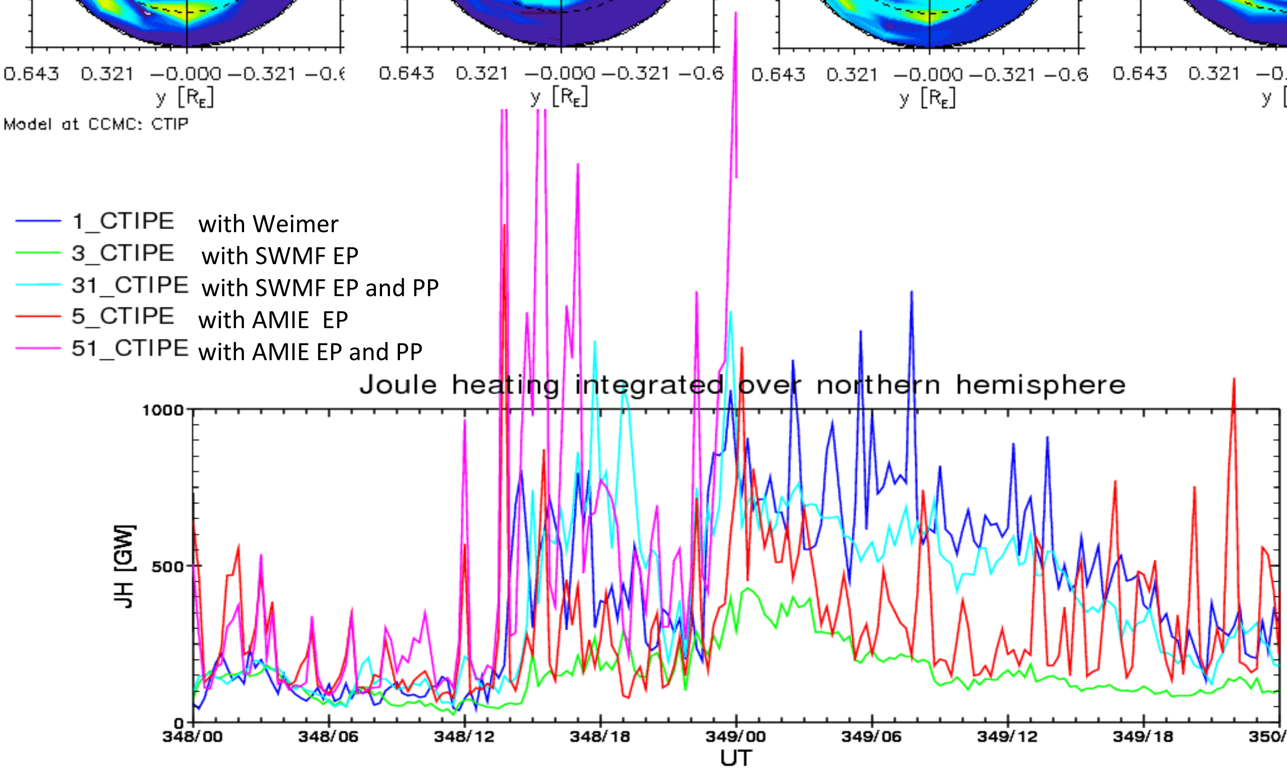


- During quiet time and recovery phase, integrated JH obtained from CTIPEs with AMIE are larger than the values from other CTIPe runs.
- After the storm onset, 1_CTIPe (Weimer05) is larger than the values from 5_CTIPe.

# Joule Heating (NH) (12/15/2006 00:00) : TIE-GCM runs

2_TIE-GCM(Weimer05) 7_TIE-GCM(AMIE) 8_TEI-GCM(SWMF) 9_TIE-GCM(CMIT)

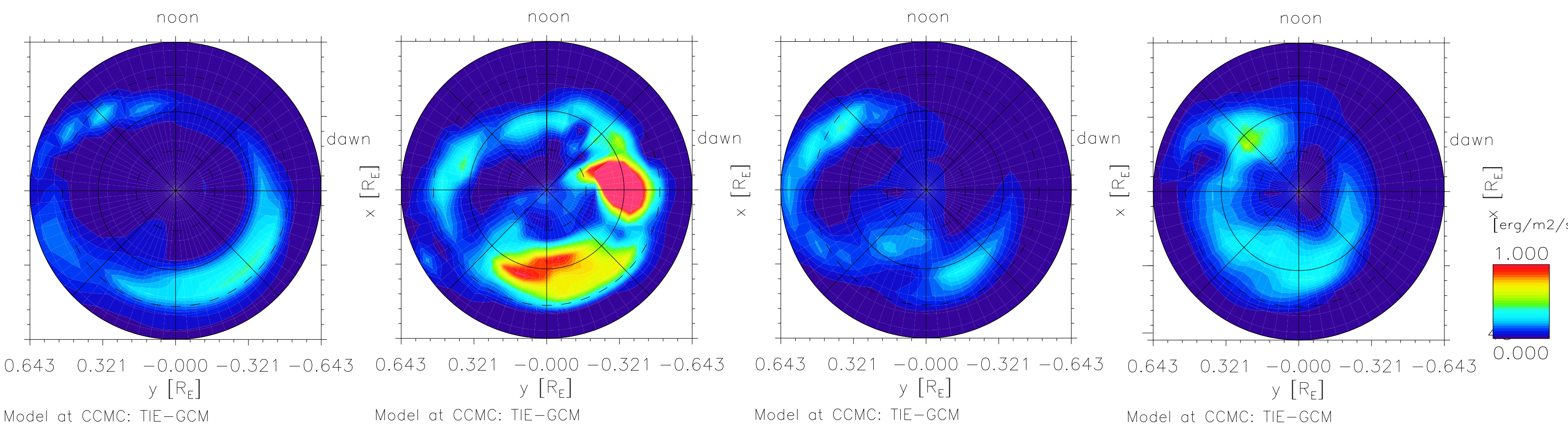


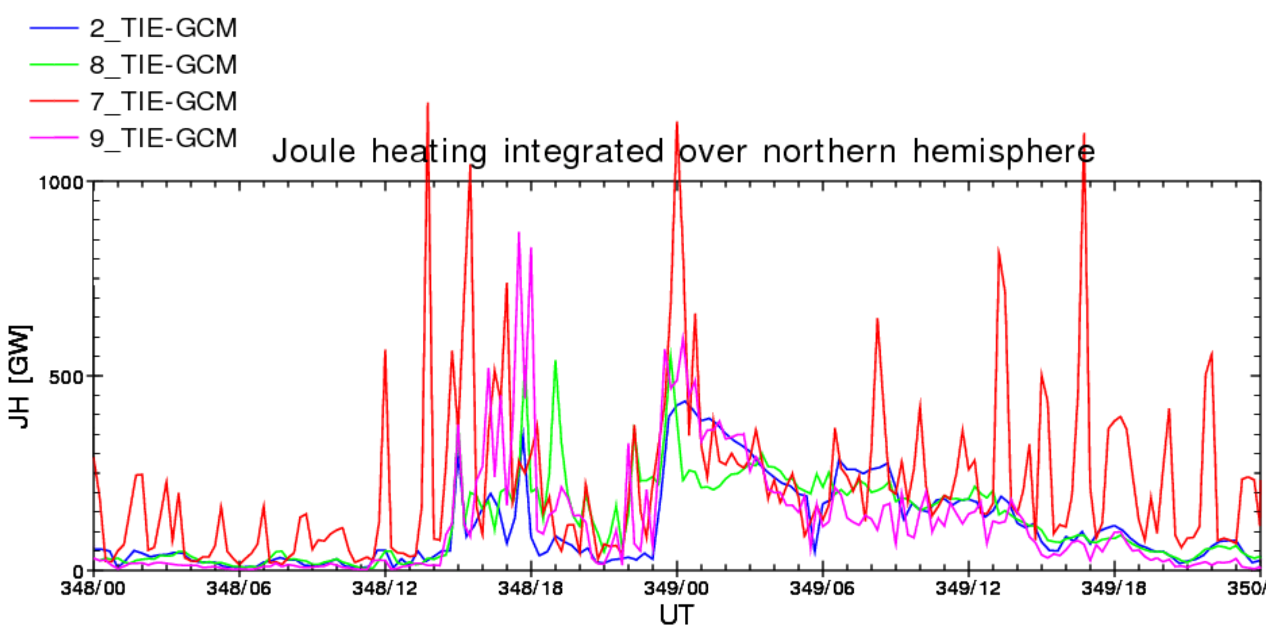


- 7_TIE-GCM (AMIE) produces the largest JH and Integrated JH.
- During quiet time, integrated JH from 7_TIE-GCM (AMIE) is larger than the values from other TIE-GCM runs.
- Integrated JH of 2 and 9_TIE-GCMs are similar to each during main and recovery phases.

# Neutral density at the CHAMP location

## CTIPe runs driven by Weimer/AMIE/SWMF

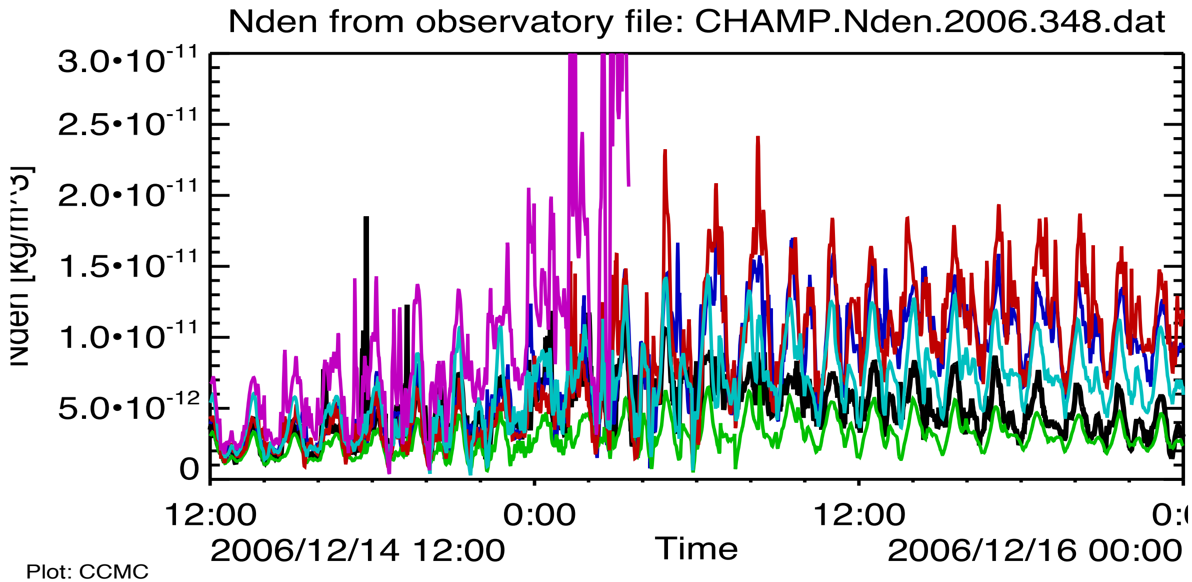


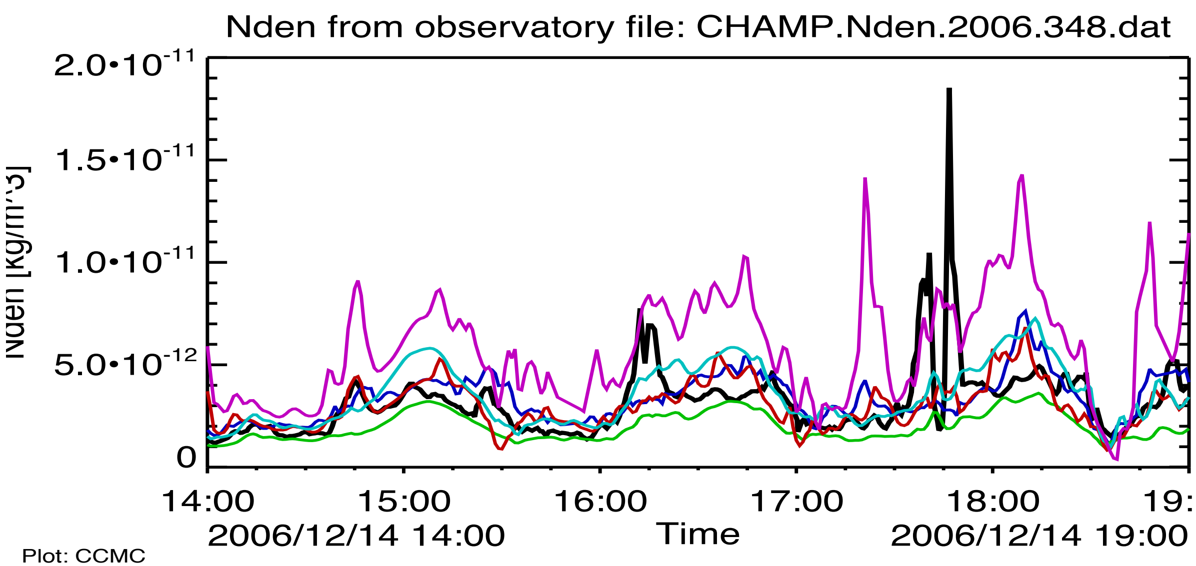


- Observation
- 1_CTIPe with Weimer
- 3_CTIPe with SWMF (EP)
- 31_CTIPe with SWMF (EP &PP)
- 5_CTIPe with AMIE (EP)
- 51_CTIPe with AMIE (EP & PP)

- In the beginning of main phase of the storm, neutral densities from 1 and 5_CTIPes show better agreement with observation than those from 3_CTIPe do.
- During recovery phase, 1 and 5_CTIPes, (which have larger CPCP than 3_CTIPe) produce larger neutral densities than CHAMP measurements and neutral density from 3_CTIPe.
- 51_CTIPe produces better density at 17:45UT on Dec. 14 than other models, but 51_CTIPe overestimates the values most of the time.

# Electron density at the CHAMP location

## Observation (CHAMP)

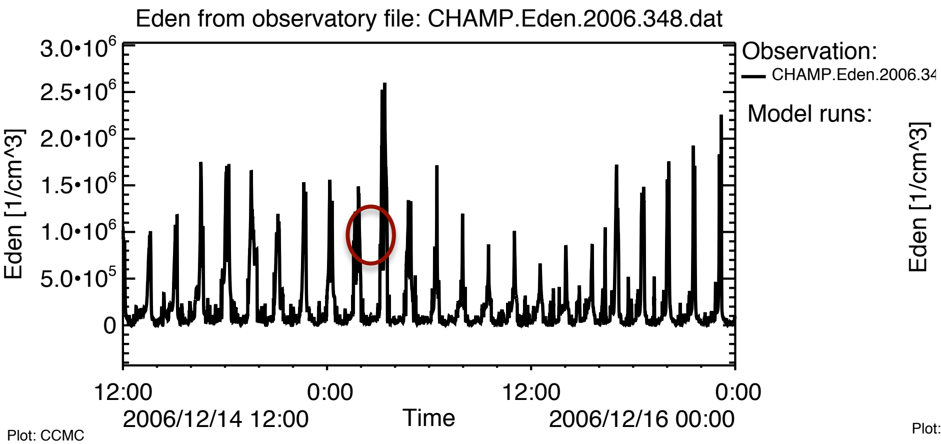


## TIE-GCM runs

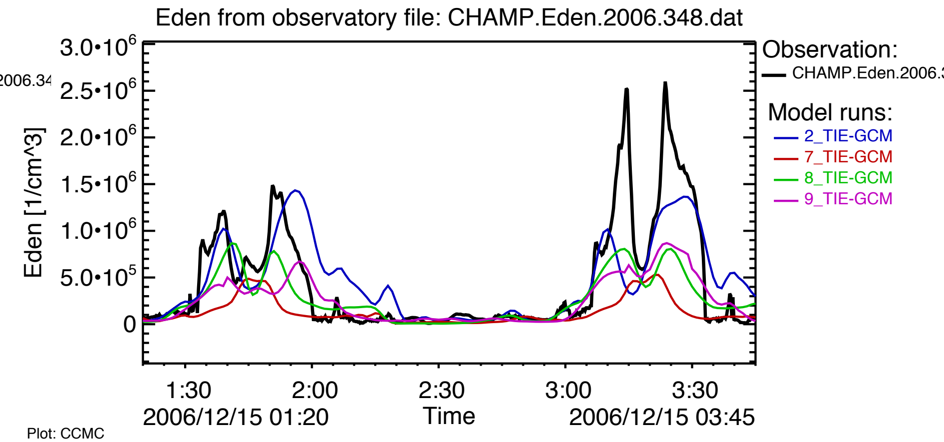


## CTIPe runs

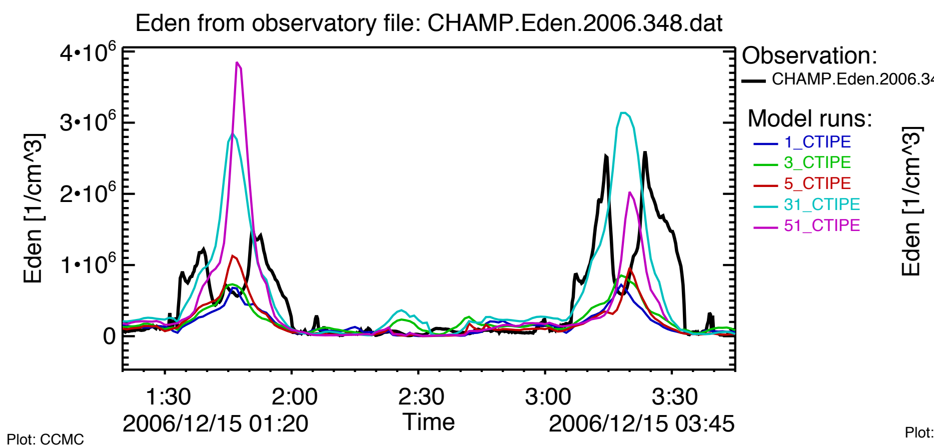


## UAM runs

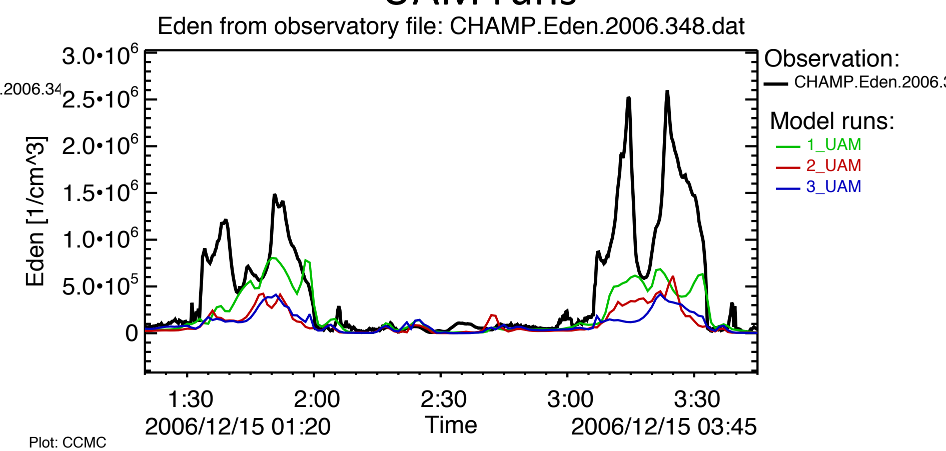

# RMS in predicting Ne

($\times 10^5/cm^3$)

low lat (0°<|lat|<25°), mid-lat (25°<|lat|<50°), high lat (|lat|>50 °)

| | low lat | mid-lat | high lat |
|---|---|---|---|
| 1_CTIPe(Weimer) | 4.37 | 2.94 | 0.97 |
| 3_CTIPe(SWMF) | 4.10 | 2.74 | 0.95 |
| 31_CTIPe(SWMF) | 8.95 | 2.74 | 1.45 |
| 5_CTIPe(AMIE) | 4.09 | 2.86 | 0.89 |
| 51_CTIPe(AMIE) | 8.87 | 3.86 | 1.14 |

| | low lat | mid-lat | high lat |
|---|---|---|---|
| 1_UAM(FAC) | 4.18 | 2.77 | 1.04 |
| 2_UAM(AMIE_UM) | 4.92 | 3.04 | 1.17 |
| 3_UAM(Weimer) | 5.14 | 3.07 | 1.13 |

| | low lat | mid-lat | high lat |
|---|---|---|---|
| 2_TIE-GCM(Weimer) | 3.70 | 2.57 | 1.58 |
| 7_TIE-GCM(AMIE) | 4.72 | 3.23 | 1.09 |
| 8_TIE-GCM(SWMF) | 3.26 | 2.14 | 1.00 |
| 9_TIE-GCM(CMIT) | 3.77 | 2.49 | 1.03 |

# RMS in predicting Neutral density ($\times 10^{-12}kg/m^3$)

| | low lat | mid-lat | high lat |
|---|---|---|---|
| 1_CTIPe | 4.39 | 4.16 | 4.44 |
| 3_CTIPe | 2.38 | 2.27 | 2.44 |
| 31_CTIPe | 2.99 | 2.32 | 2.17 |
| 5_CTIPe | 5.58 | 5.18 | 5.21 |
| 51_CTIPe | 8.68 | 5.94 | 8.79 |

| | low lat | mid-lat | high lat |
|---|---|---|---|
| 1_UAM | 9.13 | 8.29 | 6.65 |
| 2_UAM | 5.34 | 3.59 | 4.59 |
| 3_UAM | 3.63 | 3.51 | 3.75 |

- CTIPe runs with SWMF show better performance in predicting neutral density in all three latitude regions, while 5_CTIPe(AMIE) produces better Ne in low and high latitudes than other CTIPe runs.
- 1_UAM(FAC) and 3_UAM(Weimer) are the best for Ne and neutral density prediction, respectively, among UAM runs.
- 8_TIE-GCM(SWMF) shows better score in predicting Ne than other TIE-GCM runs.

# TEC and TEC Changes at 140° E

## CTIPe runs with Weimer/SWMF/AMIE

**GPS TEC (MIT)** **1_CTIPE(Weimer)** **3_CTIPE (SWMF)** **31_CTIPE (SWMF)** **5_CTIPE(AMIE)** **51_CTIPE(AMIE)**

TEC

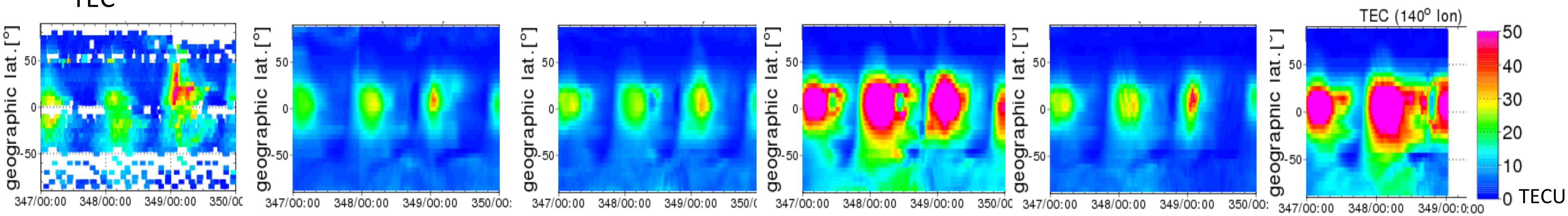


## TIE-GCM runs with Weimer/AMIE/SWMF/CMIT

**GPS TEC (MIT)** **2_TIE-GCM(Weimer)** **7_TIE-GCM(AMIE)** **8_TIE-GCM(SWMF)** **9_TIE-GCM(CMIT)**

TEC

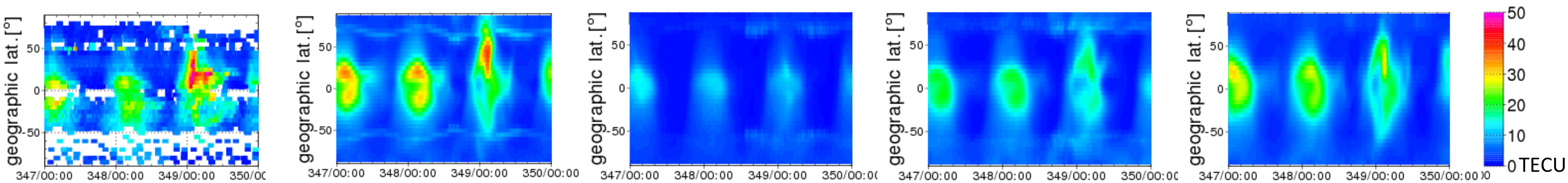

# RMS in predicting TEC

# RMS in predicting hmF2

high_s (lat < -50°), mid_s (-50° < lat < -25°), low (-25° < lat < 25°), md_n(25° < lat < 50°), high_n(lat > 50°)

| | high_s | mid_s | low | mid_n | high_n |
|---|---|---|---|---|---|
| 1_CTIPe(Weimer) | 5.587 | 10.082 | 9.804 | 5.620 | 3.345 |
| 3_CTIPe(SWMF) | 5.714 | 8.371 | 9.493 | 5.713 | 3.745 |
| 31_CTIPe(SWMF) | 9.874 | 11.771 | 20.75 | 8.335 | 3.579 |
| 5_CTIPe(AMIE) | 5.457 | 8.878 | 9.305 | 5.859 | 4.079 |
| 51_CTIPe(AMIE) | 8.577 | 10.900 | 21.74 | 8.679 | 3.557 |

| | high_s | mid_s | low | mid_n | high_n |
|---|---|---|---|---|---|
| 1_UAM(FAC) | 6.497 | 9.166 | 9.322 | 4.660 | 3.501 |
| 2_UAM(AMIE_UM) | 6.636 | 9.307 | 10.01 | 5.893 | 3.728 |
| 3_UAM(Weimer) | 6.569 | 9.487 | 9.740 | 5.712 | 3.662 |

| | high_s | mid_s | low | mid_n | high_n |
|---|---|---|---|---|---|
| 2_TIE-GCM(Weimer) | 5.425 | 9.204 | 9.266 | 9.204 | 5.425 |
| 7_TIE-GCM(AMIE) | 6.415 | 12.683 | 12.91 | 12.68 | 6.415 |
| 8_TIE-GCM(SWMF) | 5.544 | 9.737 | 9.787 | 9.737 | 5.544 |
| 9_TIE-GCM(CMIT) | 5.484 | 9.438 | 9.160 | 9.438 | 5.484 |

| | high_s | mid_s | low | mid_n | high_n |
|---|---|---|---|---|---|
| 1_CTIPe | 65.696 | 47.038 | 76.823 | 58.091 | 67.797 |
| 3_CTIPe | 59.879 | 35.813 | 84.979 | 40.472 | 49.043 |
| 31_CTIPe | 64.506 | 41.815 | 75.425 | 46.268 | 62.030 |
| 5_CTIPe | 77.790 | 50.887 | 84.681 | 64.080 | 82.576 |
| 51_CTIPe | 46.312 | 50.115 | 56.687 | 48.261 | 66.209 |

| | high_s | mid_s | low | mid_n | high_n |
|---|---|---|---|---|---|
| 1_UAM | 64.633 | 55.884 | 121.360 | 72.960 | 62.910 |
| 2_UAM | 72.554 | 98.858 | 109.070 | 96.853 | 59.847 |
| 3_UAM | 74.721 | 79.973 | 101.010 | 90.291 | 59.508 |

| | high_s | mid_s | low | mid_n | high_n |
|---|---|---|---|---|---|
| 2_TIE-GCM | 72.945 | 53.338 | 60.547 | 63.496 | 78.054 |
| 7_TIE-GCM | 91.753 | 50.469 | 57.634 | 44.511 | 38.372 |
| 8_TIE-GCM | 58.845 | 41.783 | 60.276 | 44.930 | 40.715 |
| 9_TIE-GCM | 67.773 | 55.566 | 62.435 | 71.843 | 91.906 |